



1 **3-Dimensional modeling of 2014-Malin Landslide, Maharashtra using satellite-derived data: A**
2 **quantitative approach to numerical simulation technique**

3 Shovan Lal Chatteraj¹, Prashant K. Champati ray¹, Sudhakar Pardeshi², Vikram Gupta³, Yateesh
4 Ketholia¹

5 **Affiliation:**¹Indian Institute of Remote Sensing, 4-Kalidas Road, Dehradun-248001

6 ²Univeristy of Pune, Ganeshkhind, Pune, Maharashtra-411007

7 ³Wadia Institute of Himalayan Geology, 33, GMS Road. Dehradun-248001

8

9 **Corresponding Author:**

10 Shovan Lal Chatteraj

11 Email: shovan.iitb@gmail.com

12 Phone: 0135-2524157

13

14 **Abstract:**

15 Debris flows, a type of landslides, are not nowadays limited only to the periodic devastation of the
16 geologically fragile Himalaya but also ubiquitous in weathered Deccan Volcanic Province of the
17 cratonic south Indian peninsula. Comprehensive assessment of landslide hazard, pertinently, requires
18 process-based modeling using simulation methods. Development of precipitation triggered debris
19 flow simulation models of real events are still at a young stage in India, albeit, especially in
20 tectonically less disturbed regions. A highly objective simulation technique has therefore been
21 envisaged herein to model the debris flow run-out happened in Malin. This takes cues from a high-
22 resolution DEM and other ancillary ground data including geotechnical and frictional parameters. The
23 algorithm is based on Voellmy frictional (dry and turbulent frictional coefficients, μ and ξ
24 respectively) parameters of debris flow with pre-defined release area identified on high-resolution
25 satellite images like LISS-IV and Cartosat-1. The model provides critical quantitative information on
26 flow 1) Velocity, 2) Height, 3) Momentum, and 4) Pressure along the entrainment path. The
27 simulated velocity of about 16m/s at mid-way the slide plummeted to 6.2 m/s at the base with
28 intermittently increased and decreased values. The simulated maximum height was 3.9m which
29 gradually declined to 1.5m near the bottom. The results can be beneficial in engineering intervention
30 like the construction of check dams to digest the initial thrust of the flow and other remedial measures
31 designed for vulnerable slope protection.

32 **Key Words:** landslide, debris flow, Malin, simulation, satellite image.



33 **1. Introduction:**

34 Mass wasting - a general term for all kind of movements, has become a treacherous issue in the
35 Himalaya. Quite frequently, especially during rainy season, landslides are witnessed in Lesser and
36 Central Himalaya causing severe loss to man and property. Moreover, these landslides may lead to
37 some critical problems such as blockade of rivers, which may incite secondary catastrophic disaster
38 such as floods, as was the case in 2013-Kedarnath Tragedy in the Uttarakhand Himalaya. Off late,
39 Sahyadri hills in the Western Ghats have witnessed many landslides, particularly during the rainy
40 season, causing severe loss to humankind and property (Gujarathi and Mane, 2015).

41 Considering the graveness of the issue, many researchers and experts have analyzed landslides from
42 all perspectives, i.e., to model, predict or to design preventive measures. Subsequently, the number of
43 well-tested and documented empirical methods have been evolved to determine dynamic and
44 kinematic parameters of the flow. However, some numerical simulation techniques are more
45 preferred to predict flow paths and characterize the entrainment process (Tsai et al. 2011; Quan Luna
46 et al. 2011, Evans et al. 2011). The underlying principle of such events can be applied to a variety of
47 processes including snow avalanche. Debris flows, landslides, mudflows and even rock falls and has
48 therefore found to be significant in disaster management. Although well tested empirical methods
49 adopted by Heim 1932, Scheidegger 1973, Corominas, 1996, Nicoletti and Sorriso-Valvo, 1991, Li,
50 1983, Hungr, 1995 are available to determine dynamic characteristics of a flow, numerical simulation
51 techniques, such as Hungr, 2006, Iverson, 1997, Savage and Hutter, 1989, Chen and Lee, 2000,
52 Iverson and Delinger, 2001, McDougall and Hungr, 2004, Sousa and Voight, 1991, Hungr, 1995
53 (DAN), Völlemy, 1955, Hungr and Evans, (DAN 3D), 1996, 2004, Hungr and McDougall, 2009 are
54 now being widely applied to predict flow paths and characterize the entrainment process.

55 Pertinently, as for the Indian subcontinent, the Himalayan region has experienced many devastating
56 landslides in the past. Most of the landslides in the Himalayan region have a major debris flow
57 component that travels some distance causing enormous damage enroute (Chattoraj, 2016, Chattoraj
58 and Champati ray 2015; Champati and Chattoraj, 2014). On the contrary, debris flows are less
59 abundant in Western Ghats. However, most of the works mentioned above, reports either the geo-
60 engineering aspects of landslides or hazard/ susceptibility mapping leading to damage assessment.
61 Comprehensive assessment of landslide hazard which requires process based modeling using
62 numerical simulation methods is still lacking or at nascent stage in Indian subcontinent as a whole.



63 Precipitation triggered debris flow models have, albeit, been attempted in similar tectonically
64 disturbed regions of the world and holds tremendous opportunity in implementation of a successful
65 strategy for landslide hazard mitigation (Brand 1995, Champati ray et al. 2013, Deganutti et al. 2000;
66 Hungr et al. 1987; Scott 2000). The present study aims to fill this knowledge gap by focusing on
67 numerical analysis of major landslides/debris flow movements and simulate landslides that occurred
68 in the Western Ghats. This study leads to derivation of the important physical flow parameters taking
69 cues from Earth Observation techniques to understand the root cause of the devastation, which is
70 essential for effective mitigation measures.

71 In the present study, RAMMS (Rapid Mass Movements Software) developed by WSL Institute of
72 Snow and Avalanche, Switzerland has been used, which is a state-of-the-art numerical simulation
73 model that predicts the motion of a naturally occurring mass from a head (release area) to base
74 (deposition area) in three dimensions. The present study aims to address landslides/debris flow
75 movement and simulate the landslide event that had occurred in the Malin area, the northern part of
76 the Sahyadri hill, in the wee hours of 30th July 2014 following torrential rainfall. It engulfed 40
77 houses and gobbled up 151 people as per. The event was classified as an unchanneled debris flow
78 consisting mainly of semi-consolidated, basalt-derived, silt to coarse sand-sized, poorly sorted soil,
79 highly saturated with water which was triggered by intense monsoonal precipitation on leeward side
80 of a slope underlain by thick alternating basaltic layers of varied composition and physical
81 characteristics (Champati ray and Pardeshi, 2014).

82 The outputs of such simulated flows are likely to provide the stake holders actual insight of the cause
83 of these events and associated disasters. Extensive landslide mapping at large scales complimented by
84 this kind of 3-dimensional modeling of landslides will provide adequate information to understand
85 the event and plan for the mitigation measures in future (Champati ray et al. 2013; Herva'set et al.
86 2003).

87

88 **2. Study area and location**

89

90 Malin village is located at latitude 19⁰09'40.84'' N and longitude 73⁰41'18.41'' E from 775m (avg.)
91 above MSL (SOI Toposheet no. E43B/12) on a southeasterly facing slope of a small valley oriented
92 along the NNE-SSW direction (Fig. 1). Downhill Malin village, a streamlet flows in SE direction
93 which meets Bubranadi, a tributary of Ghod river, which in turn becomes contributory to Bhima



94 river. The Bhima river system forms part of the Upper Godavari basin. The Ghod river is dammed at
95 Ambegaon forming the Dimbhe reservoir. This reservoir is fed by two significant inlets, the northern
96 one of which flows close to Malin. Besides the main Dimbhe dam, there is a small dam at 9 km
97 upstream on the Bubranadi. The upstream tail end limit of this reservoir water stops at about 1km
98 away from Malin village in the upstream direction.

99 **3. Regional Geology and Geomorphology:**

100 Geologically, the Malin and adjoining area are embedded/overlain by Deccan Volcanic Province
101 (DVP) of peninsular India consisting of numerous horizontal to gently dipping/inclined lava flows.
102 The flows are characteristically transacted by linear discontinuities like parallel joints and fractures
103 which are revealed (or reflected) in the form of lineaments and drainage systems have developed
104 (along these discontinuities). The major trend of the lineaments are observed to be NW-SE and
105 NNE/NE – SSW/SE directions (Champati ray and Pardeshi, 2014; Ramaswami et al. 2015). GSI,
106 1995 has defined three types of lava flows viz.1) fine-grained aphyric pahoehoe flows (Karla
107 Formation), 2) Aphyric to sparsely phytic flows and Megacryst flow(Indrayani Formation), 3) fine to
108 medium grained aphyric flows (Upper Ratnagarh Formation). These formations, in total,
109 accommodates 14 flows (Champati ray and Pardeshi, 2014).

110 In this area, the Sahyadri range is divided into two parts viz.1) high hills and adjoining plains located
111 in the western part and 2) denudational hills and associated river valleys (Ghod and Bhima river)in
112 the eastern part (Fig. 2). The study area falls in the second part. However, both the hill ranges show
113 extensive plateau development owing to horizontal nature of lava flows. The small valley near Malin
114 is located at an elevation of 680m, the village itself at 700-710m, followed by terrace at 750m, 800
115 and 840m on Cartosat-1 stereo-pair derived DEM. On SRTM DEM, the valley is located at 750m,
116 Malin village at 770m, the terrace at 827 and 940m. Overall the relief difference is around 160-180m
117 from the valley bottom to hilltop with an average slope of 11-13⁰, and on the steepest section, the
118 slope is 21⁰.

119 **4. Methodology and input data**

120 Multi-temporal and multi-resolution Earth Observation satellite data products and derived
121 information have been used to set parameters for flow modeling (table 1). Flow modeling has been
122 developed and validated against the actual events of 2014 by ground checking.



123 **4.1 Satellite Data used:**

124 Indian Remote Sensing Satellite data products such as LISS-IV (Resourcesat 2) data sets acquired on
125 8th January, and Cartosat-1 data acquired on 3rd March 2011 were analyzed mainly for pre-event
126 analysis (Table 1). Post-event changes were compared using LISS-IV (1st Feb 2015) and Cartosat-1
127 (6th April 2015). DEM (Res. 10m) was generated using pre-event Cartosat-1 stereo-pair in LPS
128 module of Erdas Imagine software (v. 2014). Ancillary Earth observation data like SPOT images of
129 Google Earth and terrain information derived from SRTM DEM Version 4 were also referred as
130 detailed in table1.

131 **4.2 Debris flow run-out modeling**

132 The essential dataset required for the physically based model are topographic data (digital elevation
133 model), release area and release mass as well as information on friction for dry and liquid phases and
134 geo-engineering parameters like an internal shear angle and density. Topographical data sets in the
135 form of high-resolution digital elevation model (DEM) and the location of release area are the two
136 most important parameters for flow modeling. DEM in the form of the ESRI ASCII Grid and ASCII
137 X, Y, Z format is required for implementation.

138 Debris flow modeling for unchannelized flows (as observed in the present case) requires a known
139 release area with a given initial height for block release (Rickenmann D 1999, Rickenmann, 2005;
140 Rickenmann et al. 2006). Therefore, the release areas for debris flows have been identified using
141 high-resolution satellite images (Cartosat-1 and LISS-IV) and derived DEM. The initiation zone in
142 the study area is steeper with slope angle ranging between 30-70° with height varying from 925m to
143 765m. The depth of the initiation zone (depletion zone) varies from 1m to 1.2m (Fig. 3,4). The field
144 observations revealed that the modeled landslide was initiated with weathered basalt derivatives/
145 debris and when it hit Malin village width of the slide was maximum (~150m).

146 **4.3 Frictional parameters**

147 The RAMMS numerical simulation model is based on rheological characters of the slope derived
148 from shear strength parameters of the slope. This model divides the frictional resistance into two
149 parts: a dry-Coulomb type friction (coefficient, μ) and a velocity-squared drag or viscous-turbulent
150 friction (coefficient, ξ). The frictional resistance S (Pa) is then defined as:

151 $S = \mu \rho H g \cos(\varphi) + (\rho g U^2) / \xi$



152 Where ρ is the density, g the gravitational acceleration, ϕ the slope angle, H the flow height and U the
153 flow velocity (Salm et al. 1990). The two major frictional input parameters are μ and ξ . However, it is
154 known from a law of friction that $\mu = \tan \phi$, where ϕ is an angle of internal resistance that can be
155 determined in the laboratory. In the present case, direct shear test instrument was used to determine c
156 (cohesion) and angle of internal friction from soil samples collected from the study area.

157 The main difficulty in case of debris flow simulation is the much larger variety of debris flow
158 materials, which influence the choice of the friction parameters. RAMMS Debris Flow uses a single-
159 phase model, and it cannot distinguish between fluid and solid phases, and the entire mass is modeled
160 as a bulk flow. Therefore, the friction parameters should be varied to match the observed flow paths
161 in case of known debris flow events. It is quite possible that different events in the same torrent may
162 show differences in composition. This fact makes the calibration of the friction parameters much
163 more difficult. Therefore, numbers of simulations with different values for dry and viscous turbulent
164 frictional coefficients were carried so that there is a close match between the modeled flow run out
165 and actual field/ satellite photograph observations. The results were validated with field data, and the
166 best-fitted simulation outputs were adopted for final analysis (Sosio et al. 2008).

167 Thus, some simulations were considered using various possible ranges of friction parameters. To find
168 the optimal friction values, a range of values were used. The range of dry friction ranges from 0.05 to
169 0.5 and for viscous turbulent flow is 100-800 m/s^2 (Sosio et al. 2008). Meanwhile other input
170 parameters viz. density of materials, release height, earth pressure coefficient (λ) and the
171 percent of momentum were kept constant. Afterward, validation of simulation outputs was done
172 comparing the total length of run-out distance, and the aerial extent of run out vis-a-vis the actual
173 flow paths on the ground.

174 When the simulated flow spatially matched approximately 97% (pixel-wise) with real event, model
175 parameters were frozen at μ (μ) = 0.49, ζ (ξ) = 460 m/s^2 and cohesion (c) value of 100kPa. For dry
176 friction value, it was observed from that an increase in the friction coefficient μ (μ) causes a
177 decrease in the run-out distance due to increase in the basal friction of the flow. On the other hand,
178 the value of ζ (ξ) changes did not affect the run-out distance significantly. However, in general case,
179 an increase in ζ (ξ) value increases the run-out distance and results in a relatively smoother flow.

180 Amongst RAMMS model outputs, momentum is not absolute as it simply considers momentum as a
181 product of flow height and velocity. Thus the unit is m^2/s . To get real momentum in ($\text{kg}\cdot\text{m/s}$), this



182 value is multiplied by the density of debris and area under consideration. Additionally, this numeral
183 simulation model does not include 1) en-route erosion and 2) side channel contribution to the main
184 flowing mass along run out. In most of the cases, variation in output geophysical parameters is
185 reported due to above reason. Therefore, maximum valuation of parameters has been provided with
186 error values. The outputs bound within error limits ensure that run out is restricted to the real debris
187 flow channel as verified in the field and/or satellite image.

188

189 **5. Instrumental validation of Shear strength parameters**

190 RAMMS numerical simulation derived models require cohesion (c) and the frictional coefficient for
191 dry and liquid phases (μ and ξ respectively) for soil/ debris as inputs. Cohesion is independent of
192 stress systems and is dependent more on geochemical properties of the material. Frictional coefficient
193 (static) for dry debris phase (μ) is related to the topographic slope by the rule of friction: $\tan \phi = \mu$
194 (considering the angle of sliding equal to the angle of repose). Thus, theoretically, the instrument
195 derived and modeled inputs of shear strength parameters of a successful simulation should match, if
196 assumptions are within the error range. Direct shear instrument was utilized to measure cohesion (c)
197 and angle of internal resistance (ϕ) assuming prevailing maximum in-situ saturation level. The
198 outputs of the direct shear instrument were plotted in the bivariate plot using Mohr-Coulomb
199 equation, i.e., $\tau = \sigma \tan \phi + c$ which is a straight line equation between normal and shear stress plot.
200 As each model is frozen once it approximates the real debris flow and its μ and ϕ are cross-checked
201 with the instrumentally derived c and ϕ values from the soil sample. It is to be noted that when shear
202 strength model inputs in RAMMS model and instrument derived outputs are comparable, then it is
203 considered that simulation model validates well with the real world situation.

204 The representative samples collected from the base of the flows were analyzed in electronic direct
205 shear testing equipment (Model No. AIM 104 (2kN), Make Aimil Ltd, New Delhi) at Indian Institute
206 of Remote Sensing, Dehradun at different saturation levels. Samples were tested at 0.25, 0.50 and 1
207 kgf/cm² normal load and consequent shear strength parameters at failure was calculated. The input
208 dry coefficient of friction fed in the model was thus was further crosschecked instrumentally. The
209 Mohr-Coulomb equation revealed that the cohesion (c) and angle of internal shear resistance (ϕ) of
210 semi-consolidated debris which is 98-116 KPa and 25-32° (i.e. $\mu = 0.4$ to 0.6) respectively which are
211 at par with modeled inputs.



212 **6. Results and Discussion:**

213 The debris flow reached the maximum height of approximately 3.9m near the release area (Fig. 5). It
214 consistently decreased to 1 meter with slide's propagation. However, the height suddenly rose around
215 the toe of the slide, probably to conserve momentum. The maximum velocity of about 16 m/s was
216 attained somewhere mid-way the slide. The velocity profile of the slide is zigzag with fluctuating
217 velocities. The velocity near release area was 10 m/s, which intermittently increased and decreased
218 during the entire sliding event. The velocity at toe modeled to be to be 5-6 m/s-sufficient enough to
219 bury a village! The sliding mass had maximum momentum in the lower half of the profile probably
220 due to the attainment of maximum velocity mid-way. The value of momentum near the release area
221 was around 8-9 m²/s, which then decreased and again increased to a maximum of 26 m²/s and then
222 gradually dwindled down to rest(Fig. 5).The pressure more or less followed the footprint of velocity
223 with fluctuating values throughout the landslide event. Henceforth, the maximum value of 440 KPa
224 was reached somewhere near the middle(Fig. 5).

225 This work enhanced the understanding of numerical models by studying their resemblance with real
226 landslide/debris flow that contributed to the unprecedented disaster in Malin. The vital output
227 parameters viz. velocity, height, momentum, and pressure can be used to provide insight of the event
228 and extent of runout zone of future potential flows which also helps in the understanding of slope
229 stability. Thus, this work bespeaks that numerical simulation modeling is capable of emulating
230 natural events and outputs can be used for mitigation measures. The results can be very useful in
231 engineering intervention like a construction of check dams to digest the initial thrust of the flow and
232 other remedial measures designed for vulnerable slope protection. Integrated with extensive landslide
233 mapping, 3-dimensional modeling of landslides will complimentarily provide the stakeholders actual
234 insight of the cause of this type of event vis-à-vis its effective corrective measure. The model has not
235 only produced reliable simulation results but also established the efficacy and versatility in
236 application of models in a wide range of mass wasting events about different causative factors.

237 **7. Conclusion:**

238 Three-dimensional modeling of natural debris flow events by the satellite image-based analysis
239 provided two most important results. First of all, the study provided a successful simulation of
240 selected debris flow events and generated output parameters such as velocity, height, pressure, and



241 momentum taking inputs from remotely sensed and ancillary earth observation data products.
242 Secondly, it provided critical insight into the events and their consequences. Based on the study, it is
243 concluded that the modeled flows have provided debris with sufficient height, velocity, and
244 momentum that devastated the whole area. The maximum height of the debris has been revealed to
245 approximately 4m which along entrainment path got attenuated by mainly by the change in slope.
246 However, to be on the safer side, it can be concluded that any check dam to arrest the flow and digest
247 initial thrust of the debris impact should be more than this height for this particular debris flow. This
248 study shows that rough estimation of heights of check dams for similarly vulnerable slopes can be
249 done by the development of such models in a simple but fast methodology. Spatial variation of
250 velocity and momentum of such flows can provide vital inputs to develop the design and extent of
251 remedial measures.

252 For further refinement of modeled outputs, influences of side-wise mass contribution, en-route
253 erosion, an influence of rheology and pore-pressure, relationship between discontinuity vis-à-vis
254 topography should be considered. The actual outputs can still be on the higher side as the model does
255 not include side-channel contribution and en-route erosion. Moreover, simulation output is required
256 to be verified with the previously modeled event as a part of validation strategy. In this context, the
257 input parameters are important because these parameters would affect the simulation results. Rather
258 validation was carried out on collected field data in terms of their shear strength parameters and flow
259 characteristics. In this regard to get real field data, it is always recommended to collect such data at
260 the earliest after an event.

261

262 **Acknowledgement:**

263 Contributions of students and JRFs like Shobhana, Sweta and Gopal in different phases have helped
264 immensely to shape the paper. Organizational support and overall guidance provided by Dr. A.
265 Senthil Kumar, Director, IIRS and Dr. SPS Kushwaha, Ex-Dean (Academics) are also duly
266 acknowledged. Helps received from former Director of IIRS is placed on record. SLC and PKC is
267 thankful to Indian Space Research Organization, Department of Space, Government of India for the
268 financial support provided in TDP project.

269



270 **References:**

271 Brand E.W., 1995. Slope instability in tropical areas: in Bell (ed.), Proceedings of the Sixth
272 International Symposium on Landslides, 10-14 February 1992, Christchurch, New Zealand, A.A.
273 Balkema, Rotterdam 3: 2031-2051.

274 Champati ray PK, Chatteraj SL., 2014. Sunkoshi landslide in Nepal and its possible impact in India: a
275 remote sensing based appraisal. International Archive of ISPRS, Commission VIII (WG VIII/1), pp
276 1345-1351

277 Chatteraj SL and Champati ray PK (2015) Simulation and modelling of debris flows using satellite
278 derived data: A case study from Kedarnath area. International Journal of Geomatics and Geosciences
279 6(2):1498-1511

280 Chatteraj, SL (2016). Debris Flow Modelling and Risk Assessment of Selected Landslides from
281 Uttarakhand- Case Studies using Earth Observation Data, In: Santra, A. and Mitra, S., (Eds.), Remote
282 Sensing Techniques and GIS Applications in Earth and Environmental Studies. IGI Global
283 Publication, Hershey, Pennsylvania, pp. 111-121. ISBN: 978-1-5225-1814-3.

284 Champati ray, P.K. and Pardeshi, S. 2014. Preliminary analysis of Malin landslide, Maharashtra using
285 satellite data. Indian Landslides, Vol. 7 (1 & 2), 1-8.

286 Champati ray PK, Chatteraj SL, Chand DS, Kannaujiya S (2013) Aftermath of Uttarakhand disaster
287 2013: an appraisal on risk assessment and remedial measures for Yamunotri shrine using satellite
288 image interpretation. Indian Landslides, 6 (2):61-70

289 Chen H. and Lee C.F., 2000. Numerical simulation of debris flows. Canadian Geotechnical Journal,
290 37: 146-160.

291 Corominas, J., 1996. The angle of reach as a mobility index for small and large landslides. Canadian
292 Geotechnical Journal 33: 260–271.

293 Deganutti AM, Marchi L, Arattano M (2000) Rainfall and debris-flow occurrence in the Moscardo
294 basin (Italian Alps): in Wieczorek, G.F., and Naeser, N.D., eds., Debris-Flow Hazards Mitigation:
295 Mechanics, Prediction, and Assessment: Proceedings of the Second International Conference, Taipei,
296 Taiwan, August 16-18, 2000, A.A. Balkema, Rotterdam, pp. 67-72.

297 Ering, P. and Sivakumar Babu, G.L., 2016. Probabilistic back analysis of rainfall induced landslide-A
298 case study of Malin landslide, India. Engineering Geology, 208: 154-164.

299 Evans, S.G., Hermanns, R.L., Strom, A., Scarascia-Mugnozza, G. (Eds.) 2011. Natural and Artificial
300 Rockslide Dams. Springer-Verlag, Berlin, Heidelberg, pp. 463-477. ISSN: 0930-0317



- 301 Gujarathi, P and Mane, S. J. 2015.Landslides Zones of Nearby Areas of Malin Village,Pune District,
302 Maharashtra Using GIS Techniques. International Journal of Science and Research, Vol. 4(7), 443-
303 448.
- 304 Heim, A., 1932, Bergsturz und Menschenleben, Fretz und Wasmuth, Zurich, 218 pp.
- 305 Hungr O., 1981.Dynamics of rock avalanches and other types of slope movements.Ph.D. thesis,
306 University of Alberta, Edmonton, p. 500.
- 307 Hungr, Oldrich, Morgan, GC, VanDine, DF, Lister DR (1987) Debris flow defenses in British
308 Columbia, in Costa, J.E., and Wieczorek, G.F., eds., Debris flows/avalanches: Process, recognition
309 and mitigation, Geological Society of America. Reviews in Engineering Geology 7:201-222.
- 310 Herva'set J, Barredo J.I., Rosin P.L., Pasuto A., Mantovani F., Silvano S., 2003. Monitoring
311 landslides from optical remotely sensed imagery: the case history of Tessina landslide, Italy.
312 Geomorphology 54:63–75
- 313 Hungr, O., 1995. A model for runout analysis of rapid flow slides, debris flows, and avalanches,
314 Canadian Geotechnical Journal, 32, 610–623.
- 315 Hungr O., 2006. Rock avalanche occurrence, process and modelling. In Evans S.G. et al. (eds)
316 Landslides from Massive Rock Slope Failure. NATO Advanced Workshop, Celano, Italy. NATO
317 Science Series, Springer.
- 318 Hungr O. and Evans S.G. 1996.Rock avalanche runout prediction using a dynamic model.
319 Proceedings 7th International Symposium on Landslides, Trondheim, Norway, 1: 233-238.
- 320 Hungr O. and Evans S.G., 2004. Entrainment of debris in rock avalanches; an analysis of a long run-
321 out mechanism. Bulletin, Geological Society of America, no. 9/10, 116:1240–1252.
- 322 Hungr, O. and McDougall, S. 2009. Two numerical models for landslide dynamic analysis.
323 Computers & Geosciences 35(5):978–992.
- 324 Iverson, R.M. 1997. The physics of debris flows. Reviews of Geophysics, 35: 245-296.
- 325 Iverson R.M. andDenlinger R.P., 2001.Flow of variably fluidized granular masses across three-
326 dimensional terrain. 1. Coulomb mixture theory, Journal ofGeophysical Research, 106: 537-552.
- 327 Li, T., 1983, A mathematical model for predicting the extent of a major rockfall, Zeitschrift fur
328 Geomorphologie, 27 (4): 473-482.
- 329 McDougall, S. and Hungr, O., 2004.A model for the analysis of rapid landslide motion across three-
330 dimensional terrain, Can. Geotech. J., 41, 1084–1097.



- 331 Nicoletti P.G, Sorriso-Valvo M., 1991. Geomorphic controls of the shape and mobility of rock
332 avalanches. *Bulletin of the Geological Society of America* 103 (10):1365–1373.
- 333 Quan Luna B., Blahut, J, van Westen, C.J., Sterlacchini, S., van Asch T.W.J. and Akbas, S.O. 2011.
334 The application of numerical debris flow modelling for the generation of physical vulnerability
335 curves. *Natural Hazards and Earth System Sciences* 11: 2047–2060.
- 336 Ramasamy, S.M., Muthukumar, M. and Subagunasekar, M., 2015. Malin–Maharashtra landslides: a
337 disaster triggered by tectonics and anthropogenic phenomenon, *Current Science*, 108 (8): 1428-30.
- 338 Rickenmann D (1999). Empirical relationships for debris flows. *Natural Hazards* 19: 47-77.
- 339 Rickenmann, D. 2005. Runout prediction methods. In: M. Jakob & O. Hungr (eds.), *Debris-flow
340 Hazard and Relation Phenomena*, Chichester, Springer: 305-324.
- 341 Rickenmann, D., Laigle, D, Mc. Ardell, B.W., Huebl, J. 2006. Comparison of 2d debris-flow
342 simulation models with field events. *Computers & Geosciences* 10: 241–264.
- 343 Salm, B., Burkhard, A., Gubler, H.U. 1990. Berechnung von Fließlawinen:
344 Eine Anleitung für Praktiker; mit Beispielen. *Mitteilungen des Eidgenössischen Instituts für Schnee-
345 und Lawinenforschung* 47: 1–37.
- 346 Savage S.B. and Hutter, K., 1989. The motion of a finite mass of granular material down a rough
347 incline. *Journal of Fluid Mechanics*, 199: 177-215.
- 348 Scheidegger, A. E., 1973. On the prediction of the reach and velocity of catastrophic landslides, *Rock
349 Mechanics*, 5: 231–236.
- 350 Scott K.M., 2000. Precipitation-triggered debris-flow at Casita Volcano, Nicaragua: Implications for
351 mitigation strategies in volcanic and tectonically active steep lands. Paper published in *Proceedings of
352 the Second International Conference on Debris-Flow Hazards Mitigation: Mechanics, Prediction, and
353 Assessment*, Taipei, Taiwan, August 16-18, Rotterdam, pp 3-13
- 354 Singh, TN., Singh, R., Singh, B., Sharma, L.K., Singh, R., Ansari, M.K. 2016. Investigations and
355 stability analyses of Malin village landslide of Pune district, Maharashtra, India. *Natural Hazards*,
356 April 2016, Vol. 81, (3), 2019–2030.
- 357 Sosio, R., Crosta, G. B. and Hungr, O. 2008. Complete dynamic modeling calibration for the
358 Thurwieser rock avalanche (Italian Central Alps). *Engineering Geology* 100: 11–26.
- 359 Sousa J. and Voight B. (1991) - Continuum simulation of flow failures. *Geotechnique*, 41: 515-538.



360 Tsai, M. P., Hsu, Y. C., Li, H. C., Shu, H. M. and Liu, K. F. 2011. Application of simulation
361 technique on debris flow hazard zone delineation: a case study in the Daniao tribe, Eastern Taiwan.
362 Natural Hazards and Earth System Sciences 11: 3053–3062.

363 Voellmy A (1955) Uber die Zerstorkraft von Lawinen. SchweizBauzeitung 73:212–285.

364

365 **Table Captions:**

366 Table 1 Satellite data types and its sources

367 **Figure Captions:**

368 Figure. 1 Location map of the study area (Source: Astrium, May 3, 2016, © Google Earth). (Inset:
369 study area shown in Indian map)

370 Figure. 2 Geomorphological map (1:50000) of a part of Pune District, Maharashtra (Source: Bhuvan,
371 NRSC). Black and white line represent Pune district boundary and major road network respectively.

372 Figure 3. Filed photograph and satellite imagery. (a) Panoramic view of the Malin Landslide
373 (Photograph taken on September, 2015). Field length of photograph = 250m; (b) SPOT Image, Apr,
374 03, 2015 (© Google Earth); (c) Standard FCC of LISS IV, Jan 8, 2014 (RGB:321), Resourcesat-2.
375 Black circle highlights Malin village.

376 Figure 4. (a) Subset of DEM of Malin area showing source area (in violet) and area of influence
377 (inside green boundary) of debris flow; (b) Elevation map Malin area

378 Figure. 5 Spatial variation of vital flow parameters of the debris flow model. (a) Momentum; (b)
379 pressure; (c) velocity and (d) height.



Fig. 1 Location map of the study area (Source : Astrium, May 3, 2016, © Google Earth).

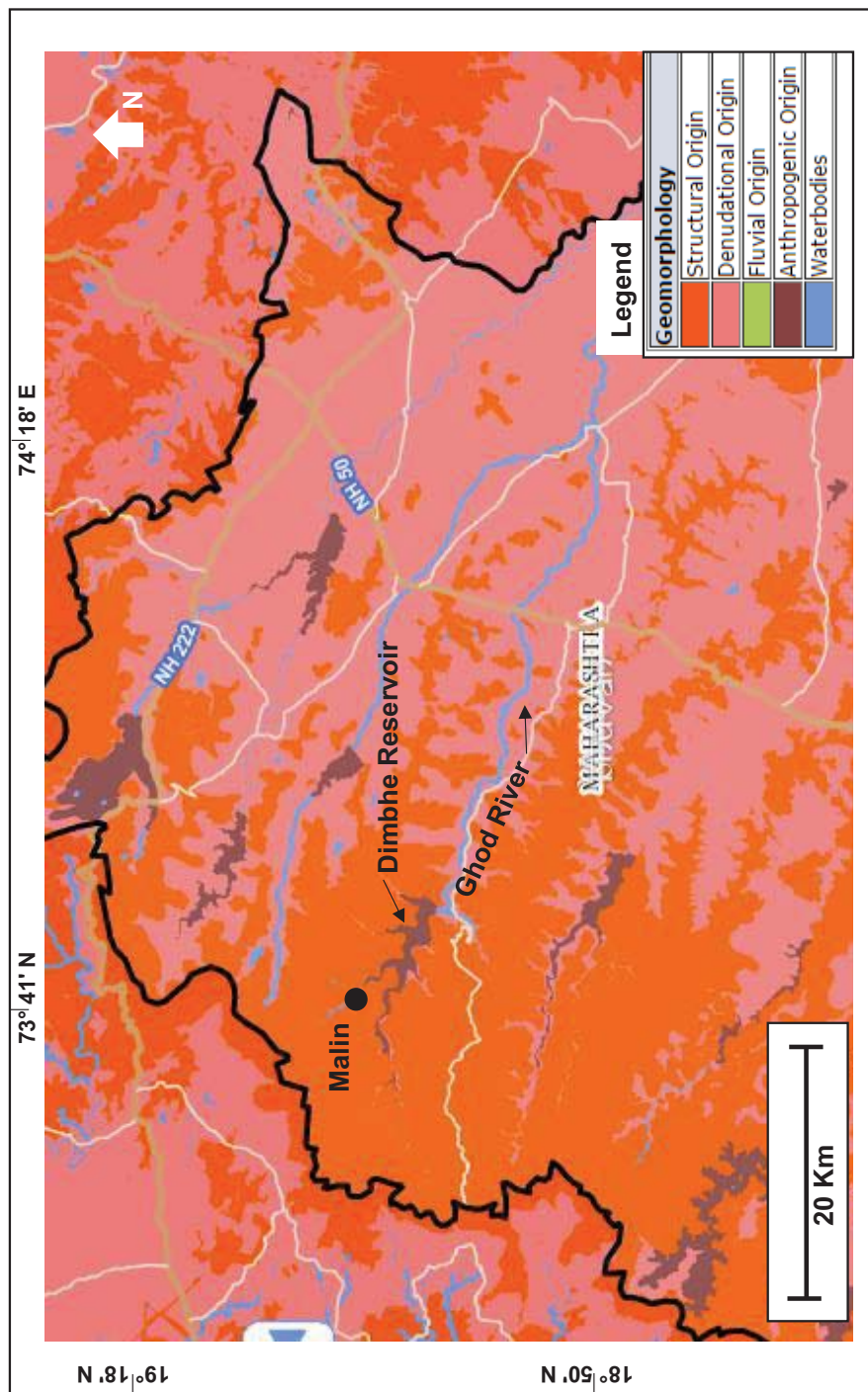


Fig. 2 Geomorphological map (1:50000) of a part of Pune District, Maharashtra (Source: Bhuvan, NRSC). Black and white line represent Pune district boundary and major road network respectively.

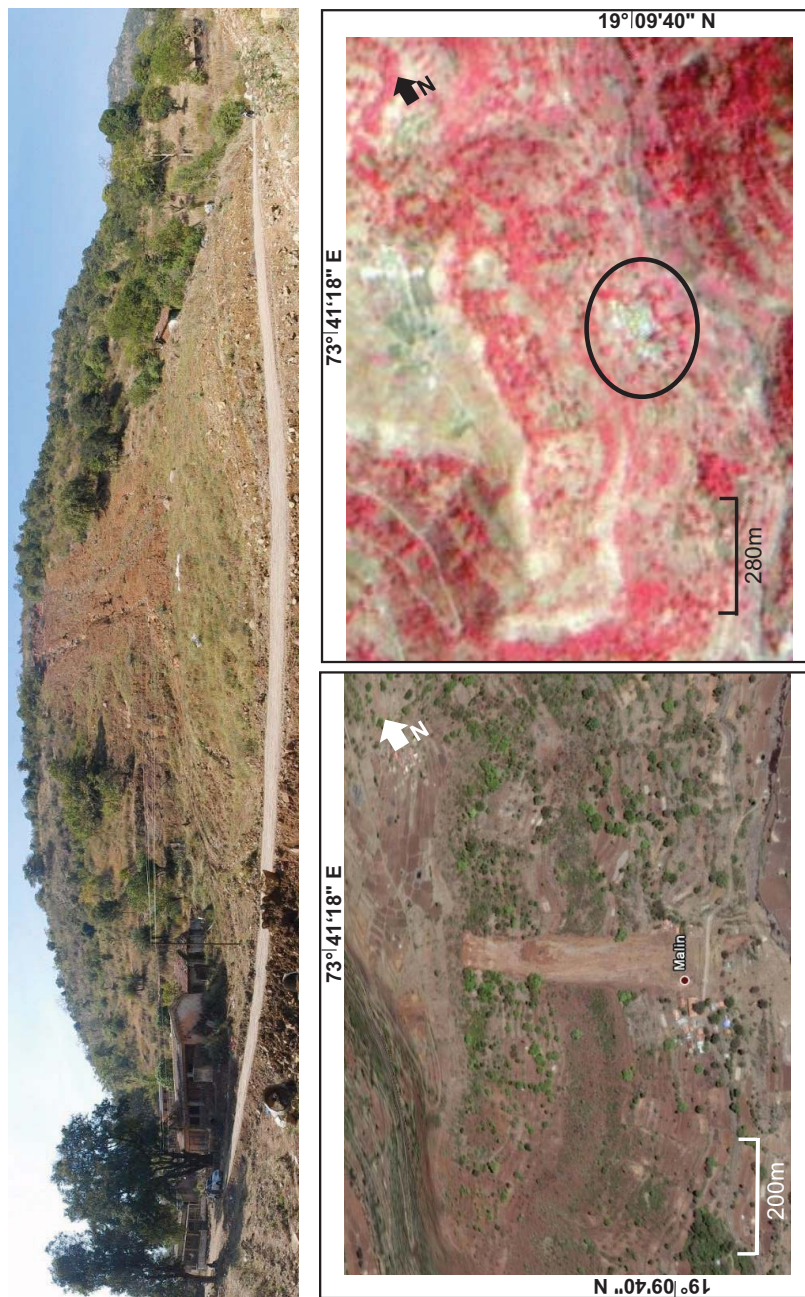


Fig. 3. Filed photograph and satellite imegray. (a) Panoramic view of the Malin Landslide (Photograph taken on September, 2015). Field length of photograph = 250m ; (b) SPOT Image, Apr, 03, 2015 (© Standard FCC of LISS IV, Jan 8, 2014 (RGB:321), Resourcest-2. Black circle highlights Malin village.

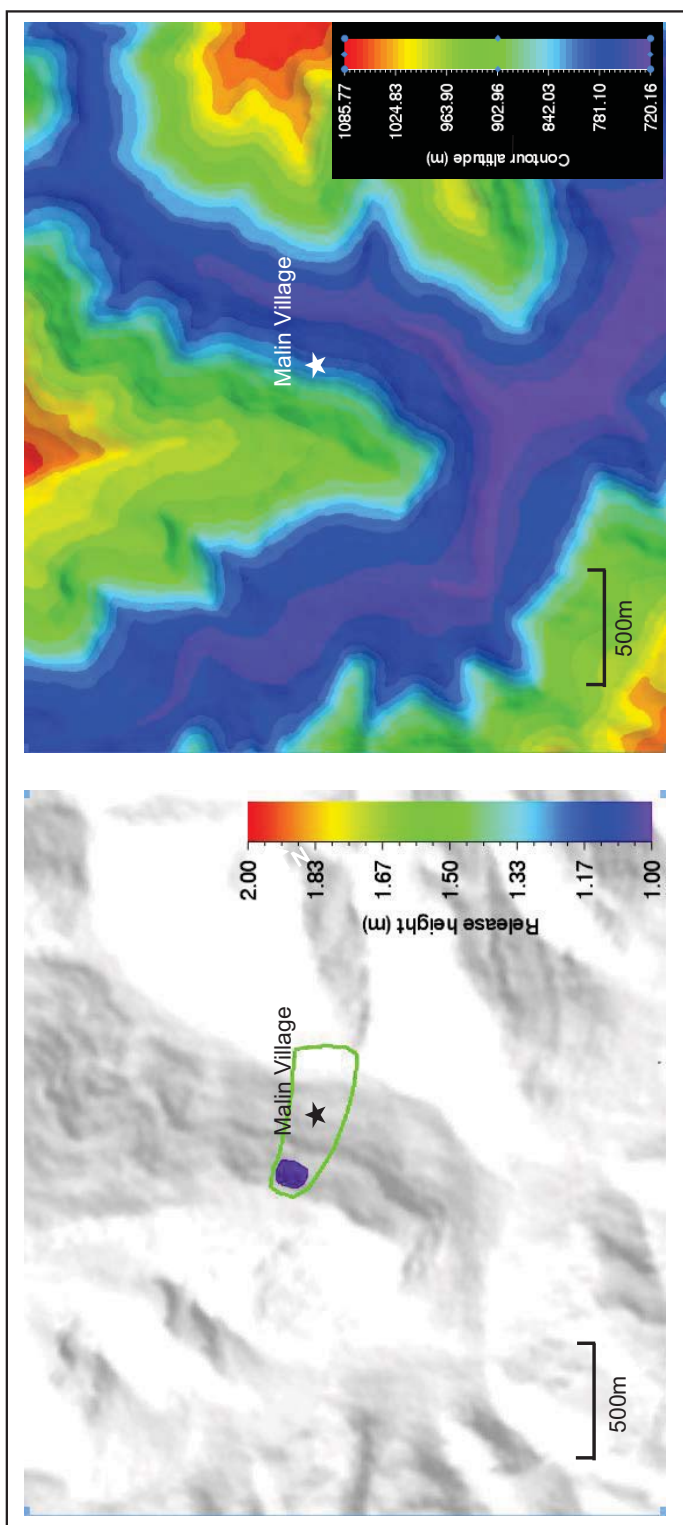


Fig. 4 (a) Subset of DEM of malin area showing source area (in violet) and area of influence (inside green boundary); (b) Elevation map Malin area.

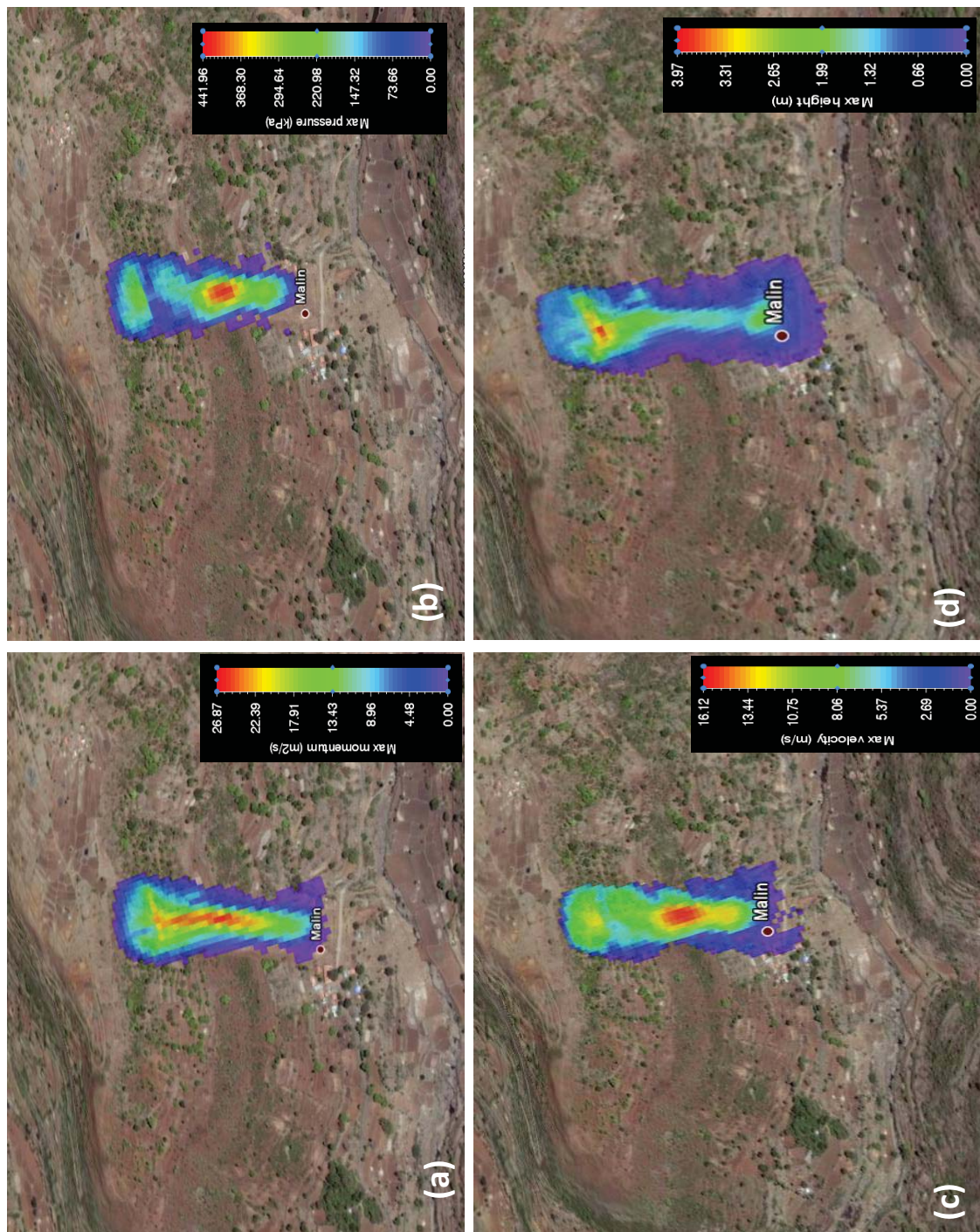


Fig. 5 Spatial variation of vital flow parameters of the debris flow model. (a) Momentum (b) pressure (c) velocity and (d) height



Table 1. Satellite data types and its sources

Data Type	Source
LISS-III, 02.12.2011 , 23.5 m resolution, 4 bands	Bhuvan, ISRO Geoportal
LISS-IV, 08.01.2011 (Pre-event) and 01.02.2015 (Post event), 5.2 m resolution, 4 bands	National Remote Sensing Centre (NRSC), ISRO
Cartosat-1, 06.04.2015 (Post event), 2.5 m, PAN	
Cartosat-1 stereo pair derived DEM, 10 m resolution (3 rd March, 2011)	Bhuvan, ISRO Geoportal
SPOT satellite image	Google Earth
SRTM DEM, 90m	USGS Earth Explorer
Topographical map (E43B/12)	Survey of India
Geological information	Reports of GSI and published papers